Available online at www.sciencedirect.com
SCIENCE DIRECT
Journal of Non-Crystalline Solids 352 (2006) 3134–3139
JOURNAL OF NON-CRYSTALLINE SOLIDS
www.elsevier.com/locate/jnoncrysol

XPS study of pulsed Nd:YAG laser oxidized Si

G. Aygun [a,b,*], E. Atanassova [c], K. Kostov [d], R. Turan [a]

[a] Department of Physics, Middle East Technical University, TR-06531, Ankara, Turkey
[b] Department of Physics, Izmir Institute of Technology, TR-35430, Urla-Izmir, Turkey
[c] Institute of Solid State Physics, Bulgarian Academy of Sciences, Sofia 1784, Bulgaria
[d] Institute of General and Inorganic Chemistry, Bulgarian Academy of Sciences, Sofia 1113, Bulgaria

Received 9 September 2005; received in revised form 28 November 2005
Available online 12 June 2006

Abstract

X-ray photoelectron spectra (XPS) of thin SiO_2 layers grown by pulsed Nd:YAG laser at a substrate temperature of 748 K are presented. The peak decomposition technique combined with depth profiling is employed to identify the composition and chemical states of the film structure. It is established that the oxide is non-stoichiometric, and contains all oxidation states of Si in different amounts throughout the film. The interface Si/laser-grown oxide is not abrupt, and the coexistence of Si_2O_3 and Si_2O suboxides in a relatively wide interfacial region is found. It is concluded that post-oxidation annealing is necessary in order to improve the microstructure of both oxide and near interface region.

PACS: 42.62.−b; 79.60.−i; 87.64.Lg; 81.65.Mq

Keywords: Silicon; Laser–matter interactions; Lasers; XPS

1. Introduction

The great success of microelectronics, during the past several decades is related with the fact that Si has native oxide that is SiO_2 – nearly ideal insulator giving practically perfect interface with Si. The continual scaling of CMOS technologies, however, has pushed the Si/SiO_2 system to its very physical limits and the development of future generations (Gigabit scale) of both Dynamic Random Access Memories (DRAMs) and MOSFETs require alternative dielectric films with a high dielectric constant, (high-κ) [1–3]. At the same time, new methods of oxidation of Si for extremely thin SiO_2 growth is still a subject of ongoing investigations [4–8]. These methods are in fact new trends in the efforts to obtain dielectric (mainly SiO_2-based) layers with enhanced capacitance properties to meet the requirements of the high density DRAMs. Among them, the techniques enabling local and low temperature oxidation are of a special interest. For example, the local oxidation by Atomic Force Microscopy (AFM) has received much attention [5,6]. At present, however, AFM-grown SiO_2 shows very poor dielectric quality compared to thermally grown SiO_2 [6] and is not suitable as an active dielectric. It is not convenient for mass production either. Despite the fact that the techniques of laser oxidation are far from their full optimization, they have a great potential for future device applications. In addition to the advantages such as local oxidation and low processing temperatures, laser-assisted oxidation provides a good control over the thickness of very thin films including SiO_2 [7,9–12]. Recently, we have reported [7,13] that the amorphous thin SiO_2 films could be successfully obtained by pulsed Nd:YAG laser in O_2 ambient at relatively low temperatures. It was established that an interval of laser beam energy density exists in which the oxidation occurs without surface melting. Electrical data of laser-oxidized SiO_2 layers have shown typical MOS behavior and the laser-grown

* Corresponding author. Tel.: +90 232 750 7637; fax: +90 232 750 7509.
E-mail address: aygun@photon.iyte.edu.tr (G. Aygun).

0022-3093/$ - see front matter © 2006 Elsevier B.V. All rights reserved.
doi:10.1016/j.jnoncrysol.2006.03.063

oxide generally has parameters close to those of thermally grown SiO_2 in terms of interfacial defect charges, slow state densities and leakage current levels. The results implied, however, that the oxide through the depth is most likely non-stoichiometric, with excess Si. It was speculated that the structural non-perfections are responsible for the detected high density of oxide charge. Obviously, the precise structural analyses are required for laser-oxidized films. It is known that X-ray Photoelectron Spectroscopy (XPS) could be successfully used to detect as well as to identify various suboxides and their distribution in the oxide and at the interface. In this article, XPS investigation of laser-oxidized SiO_2 is reported. The best oxidation conditions in terms of laser beam energy density and substrate temperature are used as determined by the capacitance–voltage and current–voltage characteristics [7]. Layers with thickness d of 40 nm were studied.

2. Experimental procedure

Chemically cleaned p-type (100) 15 Ωcm Si wafers (a standard 2:1 solution of H_2SO_4 and H_2O_2) were used as substrates. After the cleaning (including the final step of dipping into dilute HF to remove the native oxide), the samples were laser oxidized in vacuum chamber evacuated to a base pressure below 0.13 Pa. The substrate was heated to the temperature of 748 K prior to oxidation. O_2 gas was introduced into the chamber (working gas pressure, p, was 123 Pa) after reaching the desired substrate temperature. Nd:YAG laser at 1064 nm, (EKSPLA Pulsed Laser NL 301) was used to induce oxidation. The laser output is composed of a pulse train with individual pulses typically of 4.7 ns. More details on the laser parameters and the process of oxidation can be found elsewhere [7]. The approach used is only briefly described here. A computer controlled X–Y scanner system was used to direct the laser beam on a certain region on the substrate with controllable dimensions. By means of the scanner system, the laser beam was scanned over an area of the substrate of approximately $4 \times 4\ mm^2$ and it can be further reduced by the software. The laser beam energy density, P, was 3.4 J/cm^2 per pulse. The preliminary measurements showed that the small variations of P, from 3.35 to 3.45 J/cm^2, had no effect on the XPS data. According to the previous results [7], this value of P is close to the laser fluence corresponding to surface melting but without crossing it. It enables oxidation process without surface melting. The oxide thickness and refractive index of the layers obtained were measured by ellipsometry ($\lambda = 632.8$ nm). The refractive index was 1.45.

XPS was used to analyze the composition and chemical states of laser-oxidized SiO_2 film and its interface with Si. The data were obtained using an Al K_α (1486.6 eV) excitation source in ESCALAB Mk II apparatus (VG Scientific) with a residual gas pressure better than 1×10^{-8} Pa. All spectra were taken at 300 K. The photoelectrons were separated by a semispherical analyzer with a pass energy of 10 eV and an instrumental resolution of 1.0 eV measured as the Full Width at Half Maximum (FWHM) of the Ag $3d_{5/2}$ photoelectron peak. The energy position of the peaks was determined with an accuracy of 0.1 eV. The photoelectron lines of Si 2p and O 1s were recorded. The binding energies E_b have been corrected for sample charging effect with referenced to the C 1s line at 285.0 eV for the surface of the oxide, and to the Si 2p line of the elemental Si at 98.7 eV for all spectra obtained after ion sputtering. The peak positions and FWHM were determined from least square fitting using the instrument's software. The peak shapes for all peaks were fixed to a mix of Gaussian–Lorentzian functions. The final fitting was made iteratively. The composition was calculated using the standard software. The spectra were obtained under the angle of 90°, (with respect to the surface plane) of photoemitted electrons. The chamber was also equipped with an ion source to facilitate in situ sputtering of the sample by Ar^+ to determine the concentration profiles of various species. The argon ion beam was with an energy of 1.5 keV and a current density of 12 μA/cm^2. The angle of incidence of the sputtering beam was 40° with respect to the surface of the layer. The experimental curves are as-recorded data after Shirley background subtraction. It is very important to minimize the adverse effects of the ion beam on the sample stoichiometry during the ion sputtering. It is known [14] that 1–1.5 keV argon ions sputter conventional SiO_2 keeping its stoichiometric ratio, i.e., the ions remove Si and O at a rate very close to 1:2. Therefore, we assume that eventual unfavorable effects of the ion beam sputtering such as a preferential sputtering should not influence considerably the experimental results and conclusions drawn from them. During sputtering the structure of the SiO_2 layer is likely to be damaged but this is not reflected on the Si 2p binding energy or its line width. For sputtering times, t_s, of 0.5–140 min, the thickness reduction as measured by XPS [15] was linear with t_s and the sputtering rate was obtained to be 3 Å/min. The sputtering rate determined by the measured oxide thickness and t_s was approximately the same, (2.9 Å/min) indicating that both methods are correct.

3. Results and discussion

3.1. Si2p spectra

Fig. 1 presents the variation of the experimental Si 2p spectra through the depth of the films, (d_0 is the distance from the surface). The spectrum at the surface reveals a peak in the C 1s region (not shown in the figure) with negligible intensity demonstrating that the surface remains clear enough after short air exposure. The carbon signal (at 284.6 eV, indicating the presence of C–C bond) is due to adsorbate which disappears when surface is sputtered slightly, ($t_s \sim 0.5$–1 min). Fig. 2(a)–(d) illustrates spectra for several selected distances from the surface. The solid line represents as-recorded data. The peak positions extracted from the depth spectra, FWHM of the peaks

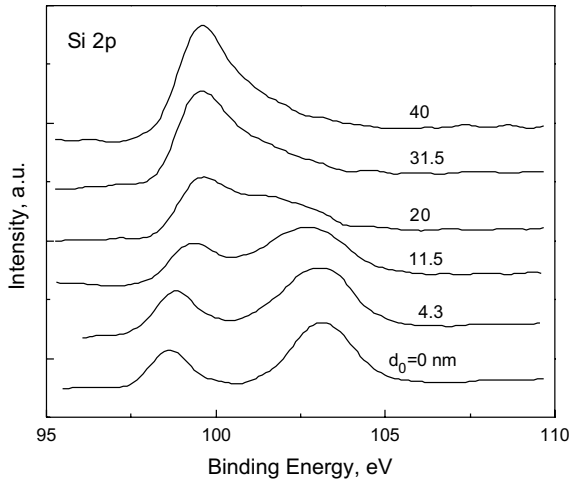

Fig. 1. Comparison of Si2p spectra for various distances d_0 from the surface.

and their shift with respect to the elemental Si line are inserted in the figures. Two symmetrical peaks could be distinguished in the spectrum at the surface: one is located at 103.1 eV, referred as Si_{2p}^{oxide}, (FWHM = 2.1 eV) which is typical position of SiO_2 [16–18] and a second lower binding energy line is located at 98.7 eV, (FWHM = 1.4 eV) referred as Si_{2p}^{Si} and associated with a signal from the substrate. The former one has a higher intensity. The analysis of the evolution of the peaks with t_s shows the following: the Si_{2p}^{oxide} line shifts to lower energy with increasing the sputtering time, (its position is 102 eV for $d_0 \sim 12$ nm); Si 2p line deforms, and Si_{2p}^{oxide} feature develops to a two-peaks-structure. At a depth of 4.3 nm from the surface, Si_{2p}^{oxide} is due to the photoelectrons from SiO_2, (or Si^{4+} according to the well known classification) and from another phase namely SiO, (or Si^{2+}). The intensity of Si^{2+} component is nearly six times smaller than that of the main SiO_2 peak. The sum of the three peaks, (elemental Si, (Si^0), stoichiometric SiO_2, (Si^{4+}) and intermediate Si^{2+} oxidation state), gives a spectrum equal to the experimental one. The Si^{4+} and Si^{2+} lines present in the spectra up to $d_0 \sim 24$ nm, but their intensities change with t_s: when thinning the oxide the intensity of stoichiometric Si^{4+} line decreases monotonously, and the intensity of Si^{2+} one increases up to a constant value in the d_0 range of 12–20 nm indicating the enhanced impact of the suboxide in the depth of the layer. The Si^{2+} peak is shifted by 2.1–1.7 eV from that of elemental Si (in dependence on d_0) which is consistent with the shift usually observed for this suboxide [17–20]. The qualitative change in the spectra is observed for d_0 greater than 20 nm, (Figs. 1 and 2): the

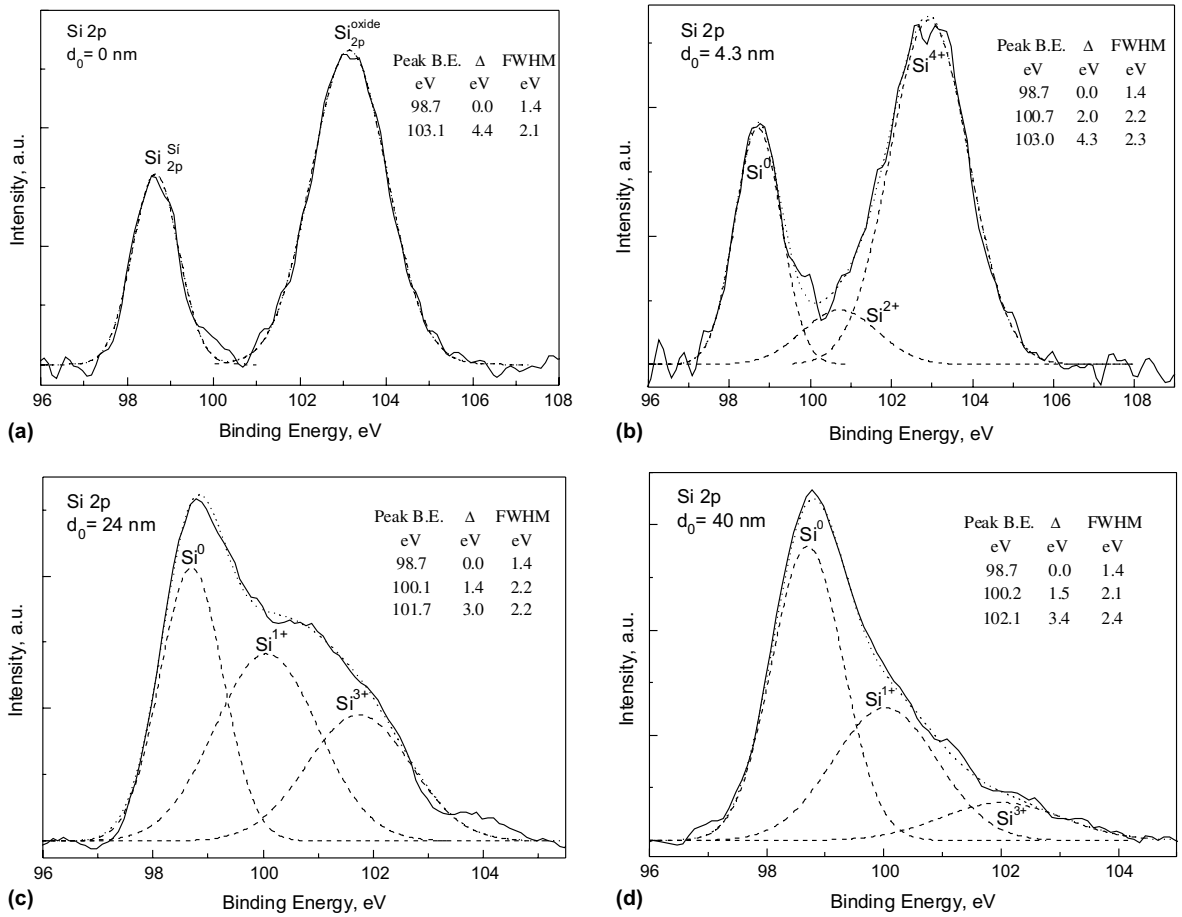

Fig. 2. Decomposition of Si2p spectra for different d_0: (a) 0 nm; (b) 4.3 nm; (c) 24 nm; (d) 40 nm; (— as-recorded data, --- decomposition of the components). The corresponding oxidation states are indicated in the figures; Δ is the energy shift of the various peaks with respect to Si^0 line.

Si_{2p}^{oxide} line changes its typical form to a broad peak with reduced intensity. The most pronounced effect of the change, however, is the missing of a SiO_2 signal for $d_0 > 24$ nm. The deconvolution of the spectra yields a set of three peaks (Fig. 2(c)) corresponding to Si^0 and two new intermediate oxidation states of Si: Si_2O, (Si^{1+}) and Si_2O_3, (Si^{3+}) [18,19]; the Si^{2+} peak disappears. The intensity variation of the different peaks towards the interface with Si is such that after $d_0 \sim 25$ nm, the peak of Si^0 dominates in the spectrum; the intensity of Si^{1+} weakly increases and Si^{3+} peak gradually loses its potency, but even just at the interface its intensity is not negligible (Fig. 2(d)). The Si^{1+} line is shifted by 1.4–1.5 eV and the Si^{3+} by 3.0–3.4 eV from that of Si^0, respectively. This is in accordance with the observations [16–20] of oxidation state peak shift of about 1 eV, (with respect to each other) starting from the line of elemental Si. The chemical shift Δ of Si^{4+} signal is 4.4 eV at the surface and nearly the same value up to $d_0 \sim 11$ nm. This value is larger than that usually obtained (3.8 eV) for thin SiO_2 films [21]. Similar values of Δ have been reported previously [22] and have been associated to structural imperfections and non-homogeneity of the layers. That is why we assigned the detected chemical shift to the presence of structural non-perfections in the laser oxidized films, i.e. strained and/or broken Si–O bonds. The nearly constant value of Δ for SiO_2 signal indicates a uniform distribution of these imperfections in the part of the layer that contains SiO_2, i.e., up to ~11 nm.

Fig. 3 in which the area under the peaks of the four oxidation states of Si as well as the area under the Si^0 peak is plotted as a function of d_0 exhibits the distribution of the observed oxidation states. The film is understoichiometric containing all possible oxidation states and their contributions depend on d_0. SiO_2 and SiO present up to $d_0 \sim 24$ nm, and SiO_2 dominates in a surface sublayer with a thickness of about 15 nm; Si_2O and Si_2O_3 suboxides present in the whole region extending from the very interface up to 15–16 nm inwards the oxide where the prevalent oxidation state is Si_2O. The quantity of each of the suboxides is constant in the near interfacial region (~8 nm from the interface); the concentration of Si_2O_3 is threefold smaller. The coexistence of these intermediate oxidation states in the interfacial region indicates a strong deviation from the ideal atomically abrupt interface. There exists excess Si in a wide interfacial transition region. If we assume that the interface with Si is defined by the ellipsometrically measured thickness of the oxide, the full width of the interfacial region is approximately 15 nm; it starts at $d_0 \sim 25$ nm and extends to the very interface where a strong increase of the elemental Si intensity is observed due to the intensification of the signal from the substrate. As is seen from Figs. 2 and 3, however, Si^0 line is in fact detected in the whole oxide layer even at the surface. It stands to a reason to interpret this peak in the depth spectra up to $d_0 \sim 25$ nm with the presence of non-oxidized Si. An alternative explanation could also be the effect of the thickness non-uniformity of the laser oxidized films, detected previously [7] in a range around beam center. The thickness profile was fitted to a Gaussian curve and the flat range (active oxidized spot on the wafer) as about 1 mm from the center across which the thickness variation is within 10%. Thus, the thickness non-uniformity could be responsible for the significant intensity of the elemental Si. A nearly constant intensity of Si^0 for $d_0 \leqslant 25$ nm is a support of this assumption. On the other hand, the presence of pinholes in the film cannot also be a priori ruled out. Films with pinholes usually exhibit a larger signal from the bulk Si, and this is exactly what we see here. If the layer is not continuous, it will give rise to an extra emission from pure Si through pinholes. In fact, no preference to any of these possible interpretations of Si^0 signal, observed in the oxide up to ~25 nm, can be given at present. However, considering the electrical and optical properties of laser-oxidized SiO_2 [7,13], we speculate that both the thickness non-homogeneity and the presence of pinholes are the most possible reasons for the observed behavior of Si^0 signal.

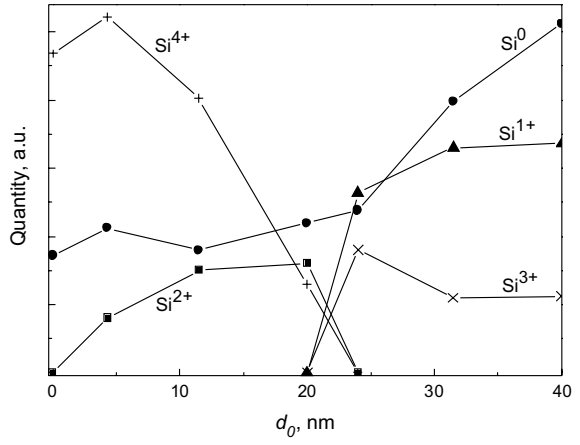

Fig. 3. Depth distribution (peak areas) of the four silicon oxidation states and the elemental silicon.

3.2. O 1s spectra

The O 1s spectrum at the surface of the sample can actually be fitted to two Gaussian components, (Fig. 4(a)). The main peak located at 532.3 eV, FWHM = 1.8 eV is close to the expected position of SiO_2 [23] but with an indication of the influence of a lower oxidation state. The line at 530.1 eV, FWHM = 1.4 eV with ~3.5 times smaller amplitude can be associated with poor oxidation state combined with surface contamination, such as carbon oxide or hydroxide. Furthermore, according to the fitting, the energy positions of these peaks are not practically changed (Fig. 4(b)–(d)). The sum of these lines, however, (i.e., the experimental O 1s peak) changes both its position and shape through the depth of the layer. Fig. 5 shows the evolution of the O 1s spectrum with thinning the film by sputtering; O 1s peak shifts to lower energy for d_0 in the range of 11–25 nm, indicating certain structural and compositional changes in the film at these depths, namely enhanced

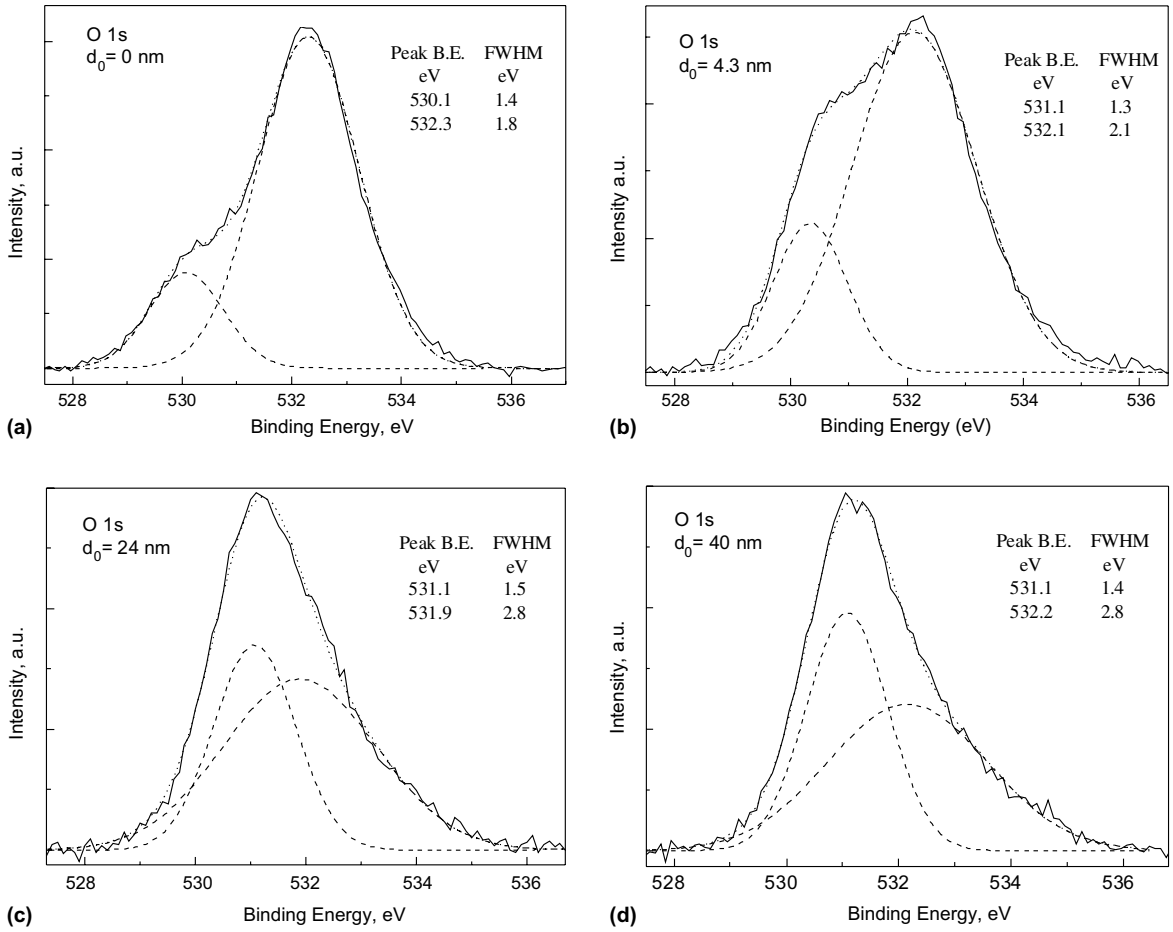

Fig. 4. O 1s spectra for different d_0: (a) 0 nm, (at the surface of the layer); (b) 4.3 nm; (c) 24 nm; (d) 40 nm; (— as-recorded data, --- after deconvolution).

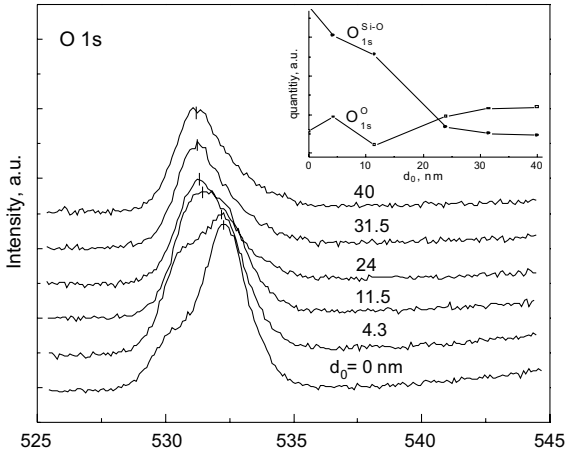

Fig. 5. Comparison of O 1s spectra for various distances from the surface. Inset shows the depth profiles of O_{1s}^{oxide} and O_{1s}^{O} peak intensities.

effect of suboxides. Subsequently, the binding energy of O 1s line is not changed up to the interface with Si. The evolution of the intensity of two peaks forming O 1s line versus d_0 is illustrated in the inset of Fig. 5. The line at 531.1 eV is assigned to the elemental oxygen [23] and we will refer as O_{1s}^{O}. The higher binding energy line, referred as $O_{1s}^{Si–O}$, dominates in the spectra up to $d_0 = 20$–22 nm, (Fig. 4) where its intensity equals to the intensity of the peak of elemental oxygen. The progressive reduction of the intensity of $O_{1s}^{Si–O}$ peak as the film is sputtered is detected, while the intensity of O_{1s}^{O} one does not change significantly suggesting the presence of elemental oxygen through the whole layer. At present we have no clear explanation for the presence of non-bridging oxygen in the laser-oxidized film. Generally there are two hypotheses for this phenomenon: (i) spontaneous decomposition of some quantity of suboxides during Ar^+ bombardment. The low energy of Ar^+ ions, (1.5 keV) enables sputtering of SiO_2 unambiguously in a stoichiometric ratio, but this energy could be high enough to decompose intermediate oxidation states especially at the places with a large amount of non-perfect bonds (dangling and/or strained bonds) as it emerged indeed in our case. On the other hand, the thickness of the surface damaged layer with altered composition as a result of action of 1.5 keV Ar^+ ions is much smaller than the information depth of take off angle used [24]. This means that the XPS signal results from the steady state region of the layer and not from the surface distorted layer. The clarification of these effects is a non-trivial task especially in such kind of non-perfect oxide which is obviously laser-oxidized SiO_2 and requires an additional precise investigation. (ii) Various structural non-perfections in

the layer including topological features and small thickness non-uniformity may introduce an additional charge shift (regardless that the peak positions in the spectra are obtained after removal of charge shift) giving an inaccurate binding energy of the XPS lines. Based on the data, however, it is not possible to accept or to reject any of these two assumptions completely.

4. Conclusion

The XPS data presented here correspond to the pulsed Nd:YAG laser oxidation of Si with a laser beam energy density close to the surface melting but without crossing it. The results imply that the laser assisted growth of SiO_2 is a promising way for obtaining of a nearly stoichiometric SiO_2 in the form of small spots with desirable thickness at low temperatures, (40 nm oxide obtained at 748 K was studied here). The composition of the oxide, however, is not uniform on the entire thickness of the layer. All possible Si oxidation states present in the film in different amount through the depth. The layer contains a dominant SiO_2 and smaller quantity of SiO in the upper half, while Si_2O_3 and Si_2O dominate completely in the wide interfacial region at Si. We speculate that the inevitable thickness non-uniformity of the layers and the eventual presence of pinholes both give rise to substantial emission and are to a great extent responsible to the behavior of Si 2p depth profiles. It is noticeable that the laser oxidation produces films with non-perfect and non-abrupt interface with Si composed of lower oxidation states (excess Si). In this scheme, one can conclude that the subsequent annealing process is absolutely needed for pulsed laser-oxidized SiO_2 layer to reduce the contribution of Si suboxides and bond-related imperfections to a tolerable level as well as to make the interface abrupt enough for device applications.

Acknowledgements

The authors acknowledge the partial financial support from TUBITAK (Scientific and Technical Council of Turkey) under the project TBAG/U68 and from Bulgarian National Science Foundation under the contract F1508.

References

[1] Intern. Techn. Roadmap for Semiconduct., SIA, San Jose, CA, Available from: <http://public.itrs.net/files2004ITRS>.
[2] E. Atanassova, T. Dimitrova, in: H.S. Nalwa (Ed.), Handbook of Surface and Interface of Materials, vol. 4, Academic Press, San Diego, CA, USA, 2001, p. 439.
[3] G.D. Wilk, R.M. Wallace, J.M. Anthony, J. Appl. Phys. 89 (2001) 5243 (and references therein).
[4] J.D. Plummer, M. Deal, P.B. Griffin, Silicon VLSI Technology, Prentice Hall, Englewood Cliffs, NJ, 2000.
[5] P.M. Campbell, E.S. Snow, Mater. Sci. Eng. B 51 (1998) 173.
[6] X. Blasco, M. Nafria, X. Aymerich, Surf. Sci. 532–535 (2003) 732.
[7] G. Aygun, E. Atanassova, A. Alacakir, L. Ozyuzer, R. Turan, J. Phys. D: Appl. Phys. 37 (2004) 1569.
[8] S. Zankovych, T. Hoffmann, J. Seekamp, J.V. Bruch, C.M. Sotomayor, Nanotechnology 12 (2001) 91.
[9] I.W. Boyd, Laser Processing of Thin Films and Microstructures, Springer, Berlin Heidelberg, 1987, Chapter 2.
[10] L. Lavisse, D. Grevey, C. Langlade, B. Vannes, Appl. Surf. Sci. 186 (2002) 150.
[11] A. Perez del Pino, P. Serra, J.L. Morenza, Appl. Surf. Sci. 197&198 (2002) 887.
[12] Q. Dong, J. Hu, J. Lian, Z. Guo, J. Chen, B. Chen, Scripta Materialia 48 (2003) 1373.
[13] G. Aygun, E. Atanassova, R. Turan, Tz. Babeva, Mat. Chem. Phys. 89 (2005) 316.
[14] J.S. Johannessen, W.E. Spicer, Y.E. Strausser, J. Appl. Phys. 47 (1976) 3028.
[15] M.H. Hecht, F.J. Grunthaner, P. Pianetta, L.I. Johansson, I. Lindau, J. Vac. Sci. Technol. A 2 (1984) 584.
[16] A.S. Vengurlekar, A.N. Chandorkar, K.V. Ramanathan, Thin Solid Films 114 (1984) 285.
[17] E. Atanassova, A. Paskaleva, Appl. Surf. Sci. 103 (1996) 359.
[18] F.J. Grunthaner, B.F. Lewis, N. Zamini, J. Maserdjian, A. Madhukar, IEEE Trans. Nucl. Sci. 27 (1980) 1640.
[19] F.T. Himpsel, F.R. Mc Feely, A. Taleb-Ibrahimi, J.A. Yarmoff, G. Hollinger, Phys. Rev. B 38 (1988) 6084.
[20] E. Atanassova, A. Paskaleva, Appl. Surf. Sci. 120 (1997) 306.
[21] C.M. Garner, I. Lindau, C.Y. Su, P. Pianetta, W.E. Spicer, Phys. Rev. B 19 (1979) 3944.
[22] T. Adachi, C.R. Helmus, J. Electrochem. Soc. 127 (1980) 1617.
[23] T.L. Barr, Appl. Surf. Sci. 15 (1983) 1.
[24] J.M. Sauz, S. Hofmann, Surf. Interf. Anal. 5 (1983) 210.